Biogeochemistry (2016) 131:321–338
DOI 10.1007/s10533-016-0281-x

Decomposition and stabilisation of Norway spruce needle-derived material in Alpine soils using a ^{13}C-labelling approach in the field

Markus Egli · Simon Hafner · Curdin Derungs · Judith Ascher-Jenull · Federica Camin · Giacomo Sartori · Gerald Raab · Luana Bontempo · Mauro Paolini · Luca Ziller · Tommaso Bardelli · Marta Petrillo · Samuel Abiven

Received: 23 April 2016 / Accepted: 21 November 2016 / Published online: 2 December 2016

Abstract Only scarce information is available on how organic C is incorporated into the soil during the decay and how (micro) climate influences this process. Therefore, we investigated the effect of exposure and elevation on the organic litter decomposition and C-stabilisation in acidic soils of an Alpine environment. An experiment with artificially ^{13}C labelled Norway spruce needles was carried out at north- and south-exposed sites between 1200 and 2400 m a.s.l. in the Italian Alps using mesocosms. After 1 year, the ^{13}C recoveries of the bulk soil were 18.6% at the north-facing slopes and 31.5% at the south-facing slopes. A density fractionation into a light (LF; $\leq$1.6 g cm^{-3}) and a heavy fraction (HF; >1.6 g cm^{-3}) of the soil helped to identify how the applied substrate was stabilised. At the northern slope, 10.5% of the substrate was recovered in the LF and 8.1% in the HF and at the south-facing slope 22.8% in the LF and 8.1% in the HF. The overall ^{13}C recovery was higher at the south-facing sites due to restricted water availability. Although the climate is humid in the whole area, soil moisture availability becomes more important at south-facing sites due to higher evapotranspiration. However, at sites >1700 m a.s.l, the situation changed, as the northern slope had higher recovery rates. At such altitudes, temperature effects are more dominant. This highlights the importance of locally strongly varying edaphic factors when investigating the carbon cycle.

Keywords Alps · Carbon stabilisation in soils · Density fractionation · Exposure · Labelled ^{13}C organic matter · *Picea abies*

Introduction

The amount of soil organic matter (SOM) is the result of net fluxes into and out of the soil (Schulze et al. 2000). These fluxes mainly depend on the primary production, SOM decomposition and its stabilisation

---

Responsible Editor: Melany Fisk.

M. Egli (✉) · S. Hafner · C. Derungs ·
G. Raab · M. Petrillo · S. Abiven
Department of Geography, University of Zurich,
8057 Zurich, Switzerland
e-mail: markus.egli@geo.uzh.ch

J. Ascher-Jenull · T. Bardelli
Department of Agrifood and Environmental Science,
University of Florence, 50144 Florence, Italy

J. Ascher-Jenull · T. Bardelli
Institute of Microbiology, University of Innsbruck,
6020 Innsbruck, Austria

F. Camin · L. Bontempo · M. Paolini · L. Ziller
Fondazione Edmund Mach, 38010 San Michele all'Adige,
Italy

G. Sartori
Museo delle Scienze, 8123 Trento, Italy

in the soil. Production and decomposition of organic matter (OM) is strongly influenced by climatic conditions. Biomass production and biological activity respond to temperature and precipitation changes (Davidson and Janssens 2006; Garcia-Pausas et al. 2007). Conceptual models assume that the stabilisation of organic carbon (OC) is achieved through physical and chemical protection of SOM (Davidson and Janssens 2006; Schmidt et al. 2011). With respect to global change, it is of great interest to identify and quantify SOM decomposition and stabilisation processes and their sensitivity to these changing climatic conditions. Forests store about 50% of carbon in the terrestrial biosphere and thus represent a large carbon pool in the global carbon cycle, even though they cover only 30% of the earth's land surface. Besides coarse woody debris (CWD) dynamics, plant-litter deposition also represents an important nutrient flux in temperate forests (Kammer and Hagedorn 2011). Depending on the plant species large amounts of the biomass are deposited as litter-fall on the soil surface. The extent that the deposited litter contributes to the soil carbon pool in the long term depends on the mineralisation rate of OC, the incorporation of OC into mineral soil by soil fauna and the leaching of dissolved OC (DOC) (Kammer and Hagedorn 2011). The decomposition patterns are related to litter quality, often characterised by the C/N ratio or its chemical composition such as the lignin content (Kammer and Hagedorn 2011). Soil-related properties—like physical and chemical soil processes such as the chemical binding of organic compounds to minerals or physical protection of SOC by aggregate formation—are responsible for the stabilisation of litter-derived products in the soil (Davidson and Janssens 2006; Schmidt et al. 2011). In addition, temperature and soil moisture also considerably influence litter decomposition. Hence, climate change can alter the biogeochemical cycle by changing the biomass production, litter decomposition and stabilisation processes in soil (Dahlgren et al. 1997; Liski et al. 2003).

Altitudinal gradient studies are particularly appropriate in the determination of the effect of the edaphic parameters. Many studies have been conducted around the globe and along altitudinal gradients to investigate SOM characteristics. Most of these studies that focused on altitudinal gradients neglected the influence of slope exposure on SOM characteristics (Dahlgren et al. 1997; Djukic et al. 2010; Garten and Hanson 2006; Murphy et al. 1998). Only a few authors took the effect of a different slope exposure on SOM dynamics into account (Egli et al. 2009; Garcia-Pausas et al. 2007). The aspect (e.g., south- vs. north-facing sites) is particularly important as it strongly influences the thermal regime in soils and surfaces.

Many studies have been conducted on litter decomposition in forests, but the applied approaches vary strongly. Kammer and Hagedorn (2011), for example, used δ^{13}C-depleted beech litter to determine litter decomposition rates. Bird et al. (2008) applied δ^{13}C- and δ^{15}N-enriched Ponderosa pine litter in temperate conifer forest soils in the Sierra Nevada. Many others determined litter decomposition rates using litter bags (e.g., Murphy et al. 1998; Liski et al. 2003). Although such studies provide litter decomposition rates, the C fluxes were only rarely partitioned (Kammer and Hagedorn 2011). While plant litters are the main source of SOM in forests, the pathways and time scales of organic C incorporation and stabilisation in soils remain mostly unclear (Hatton et al. 2012, 2015). Particularly scarce information is available for Alpine regions where thermal conditions greatly vary between north- and south-facing sites giving rise to a high variability of the population and activity of mesofauna and microorganisms and, thus, litter decomposition (Ascher et al. 2012). Consequently, our main aim was to investigate the fate of carbon deriving from Norway spruce needles during decay and its incorporation into the soil in an Alpine environment. We had the following research questions: (i) How much needle-derived carbon is recovered in the soil and included in SOM pools of the light and heavy soil fractions? (ii) What are the effects of exposure and altitudinal gradient on the carbon fluxes of decaying Norway spruce needles?

Materials and methods

Study area

The study area is located in northern Italy in the province of Trentino. The sampling sites were along an altitudinal gradient in and around Val di Rabbi (Fig. 1). In total, ten sampling sites were chosen and experimental plots (mesocosms) installed. The sampling sites N01–N05 were located on north-facing

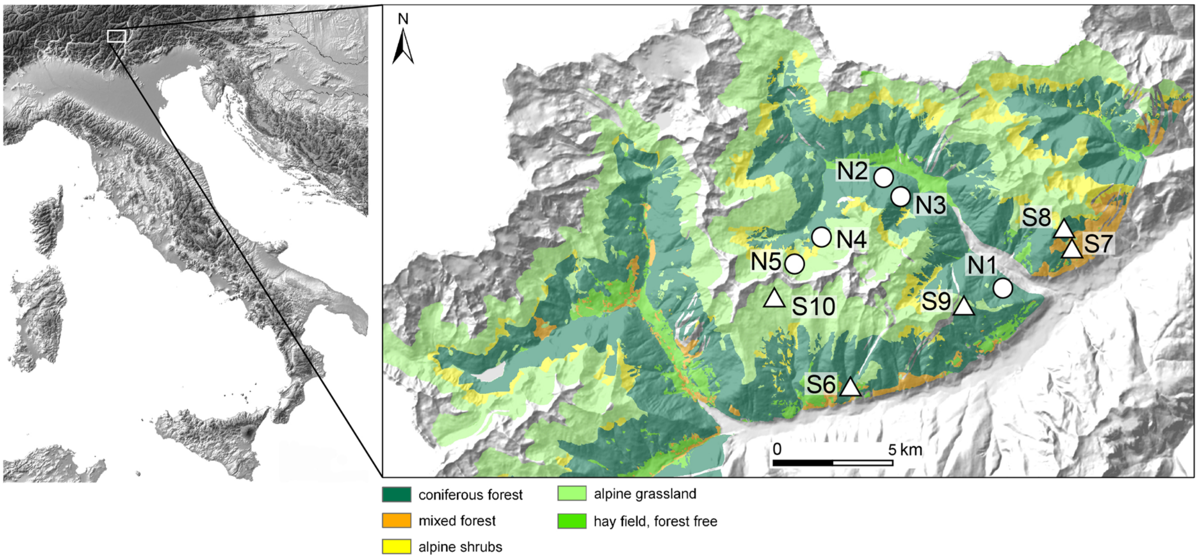

Fig. 1 Location of the study area (Val di Sole and Val di Rabbi) with major vegetation units and the investigation sites: north-facing (N01–N05) and south-facing sites (S06–S10). Data source: Museo delle Scienze (Trento), CORINE Landcover (Joint Research Center of the European Union) and scilands GmbH

slopes and the other five sites S06–S10 on south-facing slopes. The altitudinal gradient ranged from 1200 to 2400 m a.s.l. (Table 1). All sites have a siliceous parent material consisting of paragneiss (Egli et al. 2006). The sites are characterised by a subalpine/temperate (below the timber line) and Alpine (above the timber line) climate. Mean annual temperature varies from 8.2 °C in the valley floor to about −1 °C at 2400 m a.s.l. and mean annual precipitation approximately from 800 to 1300 mm (Sboarina and Cescatti 2004). Using this climosequence approach, a broad temperature range was covered having distinctly different thermal conditions. Differences in surface temperature between north- and south-facing sites in Alpine areas are usually about 2 °C (Ascher et al. 2012). The soils are variations of Cambisols and Podzols at the north-facing sites and Cambisols to Umbrisols at the south-facing sites (Table 1). Dysmoder and Hemimoder are the dominant humus forms on the north-facing slope and Hemimoder (with the occurrence of Eumesoamphi at the lowest site and Dysmoder at the highest site) at the south-facing slopes.

Experimental approach

At each site, a field experiment using soil mesocosms and ^{13}C labelled litter substrate was performed. The labelled substrate was derived from Norway spruce plants that were grown for four months in a $^{13}CO_2$ -enriched atmosphere in the MICE (Multi Isotopic labelling in a Controlled Environment) chamber at the University of Zurich (Studer et al. 2014). After 4 months, the spruce plants were harvested and dried. For the field experiments only the labelled needles were used. The measured δ^{13}C signal of the spruce needles was +43.4‰ and the organic carbon concentration of the needles 44.99%. The design of the mesocosms in the field was as described in Maestrini et al. (2014). Mesocosms (10.2 cm diam., 20 cm long PVC tubes, open at both ends) were inserted into the soil without disturbing its structure. They were not set too close to trees having thick roots. If a stone caused a problem, the mesocosm was inserted into the soil a few cm to the side. The mesocosms were installed (summer 2012) 1 year prior to the addition of the labelled substrates. In June 2013, 2 g of ^{13}C labelled, milled and homogenised Norway spruce needles substrate (*Picea abies*) was added to half of the mesocosms, the other half being used as control. The milling and homogenisation procedure ensured similar conditions for all investigation plots. The labelling experiment was performed using 4 replicates (4 label and 4 control replicates) at each site. To prevent erosion of the labelled material, the litter layer was carefully removed and the labelled substrate added on

Table 1 Characteristics of the study sites (Egli et al. 2006; Petrillo et al. 2015)

Plot ID	Elevation (m a.s.l.)	Aspect (°N)	Slope (°)	MAP[a] (mm yr^{-1})	MAAT[a] (°C)	MAST[a] (°C)	Parent material	Dominating tree species	Land use	Soil classification (WRB)	Dominant humus form (Zanella et al. 2011; Jabiol et al. 2013)
North-facing sites											
N01	1180	340	31	950	5.6	7.3	Paragneiss debris	*Picea abies*	Natural forest (ecological forestry)	Chromi-Episkeletic Cambisol (Dystric)	Hemimoder
N02	1390	0	28	1000	4.6	6.3	Paragneiss debris	*Picea abies*	Natural forest (ecological forestry)	Chromi-Episkeletic Cambisol (Dystric)	Dysmoder
N03	1620	0	29	1060	3.5	5.8	Paragneiss debris	*Picea abies*	Natural forest (ecological forestry)	Chromi-Endoskeletic Cambisol (Dystric)	Dysmoder
N04	1930	20	12	1180	1.4	5.0	Paragneiss debris, moraine material	*Larix decidua*	Originally used as pasture	Episkeletic Podzol	Hemimoder
N05	2390	30	25	1300	−1.0	2.2	Paragneiss debris		Natural grassland	Episkeletic Podzol	Dysmoder
South-facing sites											
S06	1185	160	31	950	7.6[b]	8.1	Paragneiss debris	*Picea abies*	Ex-coppice, natural forest (ecological forestry)	Episkeleti-Endoleptic Cambisol (Chromi-Dystric)	Eumesoamphi
S07	1400	145	33	1000	6.6[b]	8.7	Paragneiss debris	*Larix decidua*	Natural forest (ecological forestry)	Dystri-Endoskeletic Cambisol	Hemimoder
S08	1660	210	33	1060	5.5[b]	6.0	Paragneiss debris	*Picea abies*	Natural forest (ecological forestry)	Skeletic Umbrisol	Hemimoder
S09	1995	160	25	1180	3.4[b]	6.4	Paragneiss debris	*Larix decidua*	Ex pasture, natural forest	Skeletic Umbrisol	Hemimoder-Eumoder
S10	2420	190	28	1300	1.0[b]	4.5	Paragneiss debris		Natural grassland	Dystri-Epileptic Cambisol	Hemimoder-Dysmoder

[a] *MAAT* mean annual air temperature, *MAP* mean annual precipitation (Sboarina and Cescatti 2004), *MAST* mean annual soil temperature (at 10 cm depth)

[b] Thermally favourable conditions on south-facing sites (according to Ascher et al. 2012)

top of the soil. Thereafter, the litter layer was placed back onto the soil. Soil temperature was measured (at 10 cm depth, between July 2013 and June 2014 at 3 h intervals) by means of miniature temperature loggers (iButton®) (Schmid et al. 2012).

Soil sampling and preparation

One year after the addition of the labelled needles, the mesocosms were excavated and segmented into the sampling depths of 0–5, 5–10, and 10–15 cm. A segmentation into fixed depths does not consider the individual horizons, but it better enables a quantification and comparison between the different sites (having different horizon thicknesses). In addition, the litter layer (Ol; above 0 cm) was analysed. All samples were dried in the oven at 40 °C for 3 days. The mass of all the soil layers was measured before and after the drying period in the oven in order to obtain soil moisture during the sampling period. The samples were sieved into the fractions of >2 mm and ≤2 mm (rock fragments or fine earth) and weighed. An aliquot of the fine earth fraction <2 mm was ball-milled in a planetary mill and used to measure C and N concentrations (CHN Analyzer). The concentrations of C and N were measured using atropine having a certified percentage of C and N as reference material (Carlo Erba, Milano). Soil pH (H_2O) was determined using a soil: solution ratio of 1:10. Particle size-distribution of the <2 mm fraction was determined as a weight percentage (USDA scale) using the sieve-and-pipette method with prior oxidation of the organic matter by hypochlorite (NaClO) (Patruno et al. 1997).

Density fractionation

The soil samples (0–5 cm) were subdivided into a light- and heavy-density fraction. The light fraction (LF) had a density of ≤1.6 g cm^{-3} and the heavy fraction (HF) a density of >1.6 g cm^{-3}. The density of 1.6 g cm^{-3} was chosen as a means of achieving an optimum density cut-off in order to obtain an LF with maximum organic and minimum mineral material in it (Cerli et al. 2012). To achieve this density cut-off at 1.6 g cm^{-3}, a sodium polytungstate solution was applied. Similar to Singh et al. (2014), 250 J ml^{-1} of disruptive energy per sample was applied. Finally, all fractions were rinsed with deionised water until the electric conductivity of the sampled water solutions was below 50 µS cm^{-1}. Subsequently, all samples were dried in the oven at 40 °C for 2 days. Total C and N of all the fractions as well as the $\delta^{13}C$ were measured using a Delta Plus XP isotope ratio mass spectrometer (Thermo Finnigan) equipped with a Flash EA 1112 elemental analyser (Thermo Finnigan) at the Fondazione Edmund Mach (FEM). All the samples were analysed without treatment (or as bulk samples). They were weighed and placed into tin capsules in order to measure total $\delta^{13}C$ and the percentage of C and N in one run. The isotopic C composition was denoted in delta-ratios in relation to the international standard VPDB (Vienna Pee Dee Belemnite). The isotopic values were calculated against working in-house standards, which were themselves calibrated against international reference materials (L-glutamic acid USGS 40, IAEA-International Atomic Energy Agency, Vienna, Austria), fuel oil NBS-22 (IAEA) and sugar IAEA-CH-6 for $\delta^{13}C$). Measurement uncertainty (two standard deviations) was 0.3‰ for $\delta^{13}C$.

Calculations

Carbon stocks were calculated for the upper 15 cm according to the following equation:

$$C_{stock} = \sum_{i}^{dz} c_i \rho_i d_i (1 - RM) \tag{1}$$

where C_{stock} denotes the carbon stocks over the indicated soil depth (kg m^{-2} per 15 cm), c the organic carbon concentration (kg t^{-1}), ρ the soil density (t m^{-3}), d the thickness of the considered layers (m) and RM the mass proportion of rock fragments per sampling layer. To compare the $\delta^{13}C$ values between the control and labelled soil, a two-compartment model was applied. All observations and calculations assumed that the $\delta^{13}C$ value of the soil is mainly influenced by the $\delta^{13}C$ value of the plant leaves, since plant leaves would be deposited and transformed to SOM at a later stage (Bernoux et al. 1998). The following equation represents the two-compartment model:

$$\delta^{13}C_{labelled\_soil} = \beta \cdot \delta^{13}C_{substrate} + (1 - \beta) \cdot \delta^{13}C_{control\_soil} \tag{2}$$

where $\delta^{13}C_{labelled\_soil}$ represents the $\delta^{13}C$ value of the mixture of the $\delta^{13}C$ values of the substrate and the control soil (‰), $\delta^{13}C_{substrate}$ the δ^{13}C signal of the substrate, $\delta^{13}C_{control\_soil}$ the δ^{13}C value of the control soil and β the proportion of OC from the substrate compared to the OC of the control soil (Bernoux et al. 1998). The rearrangement of Eq. (2) allows the calculation of the substrate recovery (spruce needles):

$$sub\_rec = \frac{\delta^{13}C_{labelled\_soil} - \delta^{13}C_{control\_soil}}{\delta^{13}C_{substrate} - \delta^{13}C_{control\_soil}} \cdot 100 \tag{3}$$

where *sub_rec* represents the substrate recovery in percentage. In this experiment, the dilution effect of the substrate after addition to the soil had to be considered. A problem emerges from the fact that the soil does not have the δ^{13}C signal of the substrate at the start of the labelling experiment but rather a mixed δ^{13}C signal of the natural soil and the substrate. Therefore, the δ^{13}C signature of the labelled substrate is diluted by the natural δ^{13}C signature of the soil. This leads to an adaptation of Eq. (3):

$$\alpha = \frac{C_{substrate} m_{substrate}}{C_{substrate} m_{substrate} + C_{control\_soil} m_{control\_soil}}$$

$$1 - \alpha = \frac{C_{control\_soil} m_{soil}}{C_{substrate} m_{substrate} + C_{control\_soil} m_{control\_soil}}$$

$$\delta^{13}C_{t=0} = \alpha\delta^{13}C_{substrate} + (1 - \alpha)\delta^{13}C_{control\_soil}$$

$$sub\_rec = \frac{\delta^{13}C_{labelled\_soil} - \delta^{13}C_{control\_soil}}{\delta^{13}C_{t=o} - \delta^{13}C_{control\_soil}} \cdot 100 \tag{4}$$

where *sub_rec* means substrate recovery in percentage, *c* the SOC concentration of the indicated soil samples, *m* the mass of the mentioned samples and $\delta^{13}C$ the isotopic ratio of the indicated soil samples. $\delta^{13}C_{t=0}$ represents the δ^{13}C signal resulting from the mixing of the substrate with the natural soil at the point of time ($t = 0$) when the substrate was applied to the soil.

A potential priming effect, due to the addition of organic material, was calculated using (Fontaine et al. 2004; modified):

$$PE_{stock} = m_{control\_soil}((C_{label} - C_{rec}) - C_{control}) \tag{5}$$

where PE_{stock} = priming effect calculated on the C-stocks (kg m^{-2}), C_{label} = the SOC concentration in the labelled soil sample, C_{rec} = recovered amount of labelled substrate in the soils calculated as C concentration of the soil and $C_{control}$ = the SOC concentration in the control sample. When PE_{stock} was negative, more soil carbon had been lost during the experiment (due to an increased decomposition rate of native organic matter).

Statistical analysis

All statistical analyses were performed using the software R (3.2.3). For visualisation, the ggplot2 package was used. To test for a normal distribution, the Shapiro–Wilk test was applied. If the test indicated a normal distribution, a *t* test or an analysis of variance (ANOVA) was carried out to compare the sample sets for differences (e.g., along the altitudinal gradient or between north- and south-facing sites). In the case of non-normal distribution, the Mann–Whitney or Kruskal–Wallis tests were used. All statistical tests were performed using a level of significance of 0.05.

To explain the data distribution of ^{13}C recoveries, explanatory variables such as altitude, exposure (north vs. south), air temperature, precipitation, soil moisture, soil temperature, org. C, N, the C/N ratio, soil temperature, the amount of silt and clay, soil moisture, soil-pH, mean annual temperature (MAAT) and annual precipitation (MAP) were used. For several parameters, however, only one measurement or one series of measurements (altitude, exposure, air temperature, etc.) exist. Instead of a mixed linear modelling, we decided for a particular type of correlation analysis. To avoid autocorrelation, one replicate out of the three data points of each site (10) was chosen arbitrarily and correlated to the explanatory variables. By permutation, only one value per site was chosen. For each correlation 3^{10} combinations (i.e., a total of 59,049) were possible. In consequence, a high number of permutations and subsequent correlations could be calculated and the stability of the model tested. We performed 100 correlations for each dependent and explanatory variable and displayed the corresponding standard deviation of the correlation coefficients. The relationship between the explanatory variables and ^{13}C recovery are shown in cross-plots. This procedure does not allow the calculation of a significance level, but trends can be detected. In addition, a subdivision into south- and north-facing sites was done giving rise to 3^{5} permutations.

Results

General soil properties

The mean annual soil temperature varied at the northern gradient between 2.2 and 7.3 °C and at the southern gradient between 4.5 and 8.7 °C (Table 1). Both aspects exhibited decreasing mean annual soil temperatures with increasing altitude. Overall, the north-facing sites had distinctly ($p < 0.001$) lower soil temperatures than the south-exposed sites. Average soil temperatures at the north-facing sites were 5.3 °C and at the south-facing sites 6.8 °C. Along both altitudinal gradients, the SOC concentration reached the maximum values at an intermediate altitude (around 1650 m a.s.l) (Table 2). In general, the SOC concentrations along the northern sequence were slightly higher than on the southern slopes, although the differences were not statistically significant. Furthermore, due to the cooler and moister conditions, the north-facing sites were more acidic ($p < 0.01$; lowest pH at the intermediate altitude) than the south-facing sites. The nitrogen concentration for most of the soil depths of the northern sites showed maximum values at low and medium altitudes (1400 and 1650 m a.s.l.). The C/N ratio of both altitudinal sequences and for most of the investigated soil depths increased towards the altitude of 1650 m a.s.l. and declined at higher sites (N04 and N05, S09 and S10) (Table 2). The upper 0–5 cm layer did not show significant differences in the C/N ratio between north- and south-facing sites. The 5–10 and 10–15 cm layers, however, revealed distinctly lower C/N ratios at the south-facing slopes compared to the north-facing slopes (5–10 cm: $p = 0.003$; 10–15 cm: $p = 0.001$). The SOC stocks (0–15 cm) ranged between 4.4 ± 0.54 and 9.0 ± 1.20 kg m^{-2} and increased with altitude (Fig. 2). The average SOC stocks at the north-facing slopes were 7.5 ± 0.7 kg m^{-2} and those at the south-facing slopes 7.0 ± 0.4 kg m^{-2}. The differences between the two aspects were consequently rather small. The SOC stocks, however, differed along the altitudinal gradients: at the north-facing sites, the SOC stocks reached a maximum at an elevation of 1400 m a.s.l., whereas the SOC stocks of the south-facing sites increased steadily from the lowest to the highest site. Typical for Alpine soils, the proportion of soil skeleton (rock fragments) was substantial and showed values up to 50% in weight.

Isotopic signatures and substrate recovery

Most of the labelled plots (0–5 cm depth) differed in their $\delta^{13}C$ signal from the control plots (Fig. 3a, b). Along the north-facing slope, the average $\delta^{13}C$ signal of the control samples (0–5 cm) was −26.8 ± 0.09‰ and that of the labelled samples was 0.5 ± 0.19‰ less negative than the control samples (Fig. 3a). The control samples of the southern slopes had a mean $\delta^{13}C$ value of −27.0 ± 0.19‰ and the labelled samples were on average 1.1 ± 0.16‰ less negative than the control samples (Fig. 3b). Except for N02, all sites had a significantly less negative $\delta^{13}C$ value after the labelling experiment. Below 5 cm, no differences could be detected anymore. It seems that—if ever—only a small part of the added ^{13}C was leached into greater depths. Furthermore, with increasing depth the label signal is increasingly diluted.

The northern altitudinal sequence was characterised by low ^{13}C recoveries (Fig. 3c) at the lower altitudes (N01, N02 and N03; average values 0–9%) and high ^{13}C recoveries at the (sub) Alpine sites (N04 and N05; average values 24–57%). In contrast, the southern altitudinal transect showed rather high substrate recoveries at the lower elevated sites (S06, S07 and S08; average values 31–58%) and smaller recoveries at higher altitudes (S09 and S10; average values 14–17%). After 1 year, the average $\delta^{13}C$ recoveries of the bulk soil were 18.5 ± 5.3% at the north-facing sites and 31.5 ± 5.3% at the south-facing sites. Due to the sampling procedure, it might have been that some of the labelled material remained in or was transferred into the litter layer. However, averaging over all sites, the ^{13}C values (litter layer) of the control sites (−27.45 ± 0.11‰) did not significantly differ from the litter layer of the labelled sites (−27.31 ± 0.13‰). At the north-facing sites the litter of the control and labelled sites had identical values (−27.52 ± 0.15‰ vs. −27.54 ± 0.14‰). At the south-facing sites a small but insignificant difference between labelled and control sites was measured (−27.37 ± 0.14‰ vs −27.08 ± 0.22‰). Only at the uppermost site (S10), some labelled material seemed to persist in or be transferred into the litter layer.

The ^{13}C recovery rates seemed dependent on several environmental parameters (Fig. 4; Table 3). In general, the north-facing sites showed a (negative) correlation between the overall ^{13}C recoveries and soil and air temperature while the south-facing sites did not

Table 2 Soil properties of the climosequence (each site: n = 8, with mean and SE)

Plot	Depth (cm)	Sand (%)	Silt (%)	Clay (%)	Bulk density (g cm^{-3})	Skeleton (weight-%)	pH (H$_2$0)	Soil moisture (weight-%)	SOC (g kg^{-1})	N tot (g kg^{-1})	C/N ratio
N01	0–5	57	28	16	0.55 (0.11)	33 (7)	5.27 (0.02)	30.8 (4.7)	149.9 (22.9)	7.02 (0.67)	20.9 (1.7)
N01	5–10	46	36	18	0.85 (0.12)	45 (5)	5.26 (0.09)	26.0 (4.1)	68.1 (12.8)	3.83 (0.51)	17.2 (1.7)
N01	10–15	44	39	17	0.81 (0.08)	41 (7)	5.12 (0.09)	23.4 (5.4)	43.6 (6.9)	3.00 (0.39)	14.7 (1.2)
N02	0–5	41	39	20	0.30 (0.08)	13 (3)	4.54 (0.20)	42.3 (3.6)	261.8 (59.9)	9.86 (1.96)	25.1 (2.2)
N02	5–10	38	43	20	0.62 (0.14)	26 (6)	4.32 (0.09)	42.7 (5.2)	133.4 (41.6)	5.20 (1.34)	23.4 (2.5)
N02	10–15	39	42	19	0.67 (0.12)	15 (7)	4.58 (0.05)	n.d.	191.7 (61.8)	6.87 (1.98)	27.1 (2.5)
N03	0–5	52	26	22	0.30 (0.11)	27 (7)	4.39 (0.07)	47.9 (2.7)	303.6 (52.1)	9.91 (1.51)	30.0 (1.6)
N03	5–10	51	37	12	0.58 (0.12)	32 (5)	4.03 (0.03)	43.3 (3.7)	147.5 (47.1)	5.10 (1.14)	25.4 (2.6)
N03	10–15	53	32	16	0.68 (0.14)	25 (21)	4.03 (0.03)	n.d.	126.0 (73.0)	4.64 (1.80)	23.3 (5.1)
N04	0–5	62	24	14	0.64 (0.05)	3 (1)	5.61 (0.07)	58.0 (3.8)	90.0 (6.3)	7.26 (0.45)	12.4 (0.7)
N04	5–10	56	27	17	0.85 (0.06)	6 (1)	5.08 (0.05)	59.9 (2.9)	66.8 (5.2)	5.15 (0.45)	13.3 (0.9)
N04	10–15	68	25	7	0.85 (0.04)	8 (3)	4.91 (0.15)	57.0 (5.9)	56.9 (6.7)	3.85 (0.60)	15.8 (1.4)
N05	0–5	61	18	20	0.45 (0.03)	33 (5)	5.10 (0.08)	52.6 (5.0)	200.4 (15.4)	9.83 (0.64)	20.3 (0.6)
N05	5–10	55	28	16	0.79 (0.12)	50 (7)	4.95 (0.10)	47.3 (4.3)	129.7 (13.4)	6.79 (0.68)	19.2 (0.7)
N05	10–15	53	27	20	0.85 (0.05)	46 (6)	5.05 (0.09)	52.8 (6.6)	101.8 (10.9)	4.96 (0.55)	20.8 (0.9)
S06	0–5	57	29	13	0.49 (0.03)	15 (2)	5.76 (0.07)	33.9 (4.2)	126.7 (17.2)	6.42 (0.76)	19.4 (0.5)
S06	5–10	56	31	13	0.98 (0.04)	33 (3)	5.37 (0.04)	26.4 (3.4)	33.9 (2.2)	2.80 (0.19)	12.6 (1.4)
S06	10–15	56	31	13	1.21 (0.09)	36 (3)	5.11 (0.02)	24.5 (3.6)	16.3 (2.2)	1.89 (0.14)	9.0 (1.4)
S07	0–5	41	47	12	0.49 (0.05)	20 (5)	5.62 (0.04)	13.3 (1.3)	126.3 (13.7)	5.94 (0.62)	21.6 (1.2)
S07	5–10	63	23	14	0.82 (0.06)	27 (4)	5.62 (0.05)	14.7 (1.4)	61.6 (5.3)	4.24 (0.20)	14.6 (1.2)
S07	10–15	58	39	3	0.87 (0.05)	26 (4)	5.49 (0.05)	n.d.	44.7 (3.1)	3.50 (0.21)	13.0 (1.2)
S08	0–5	62	23	15	0.38 (0.07)	14 (4)	5.46 (0.10)	34.0 (3.5)	234.9 (34.9)	8.79 (1.10)	25.8 (1.1)
S08	5–10	42	41	17	0.61 (0.07)	14 (2)	5.61 (0.04)	30.4 (3.5)	92.5 (14.7)	4.24 (0.59)	21.7 (1.3)
S08	10–15	n.d.	n.d.	n.d.	0.74 (0.04)	16 (3)	n.d.	n.d.	53.5 (4.0)	2.62 (0.23)	20.6 (0.6)
S09	0–5	47	29	24	0.46 (0.04)	4 (1)	5.25 (0.05)	45.8 (5.1)	145.9 (10.6)	8.73 (0.51)	16.6 (0.4)
S09	5–10	48	29	23	0.68 (0.03)	5 (2)	5.08 (0.07)	48.7 (3.5)	82.2 (4.1)	5.46 (0.30)	15.1 (0.3)
S09	10–15	48	30	21	0.73 (0.03)	5 (1)	5.17 (0.07)	49.1 (4.0)	66.9 (2.6)	4.55 (0.16)	14.7 (0.4)
S10	0–5	62	23	15	0.46 (0.04)	3 (1)	5.24 (0.05)	59.1 (7.0)	150.5 (12.1)	9.34 (0.68)	16.1 (0.4)
S10	5–10	55	26	20	0.76 (0.05)	2 (1)	5.09 (0.08)	65.0 (7.0)	86.5 (6.8)	6.05 (0.44)	14.3 (0.5)
S10	10–15	54	27	19	0.91 (0.08)	13 (5)	5.20 (0.04)	56.0 (3.3)	58.1 (9.6)	4.30 (0.45)	13.1 (0.7)

n.d not determined

(Table 3). When comparing the ^{13}C recoveries with annual precipitation, then north- and south-facing sites again showed an opposing trend: the higher the MAP, the lower the recovery at south-facing sites (at north-facing sites it was the contrary). Stabilisation of organic matter is not only related to climatic conditions, but also to the grain size and the pH of the soil. Both parameters correlated with OM decay (Fig. 4; Table 3).

Density fractions and isotopic composition

At the lower sites, a high proportion of C was measured in the light fraction (Fig. 5a). This was the case for both exposures. At the subalpine and Alpine sites (N04, N05, S09, S10) a large part of C (and similarly also N) was in the heavy fraction: a trend that is probably also related to the transition from forest to Alpine grassland. C/N ratios of light and heavy fractions at both altitudinal

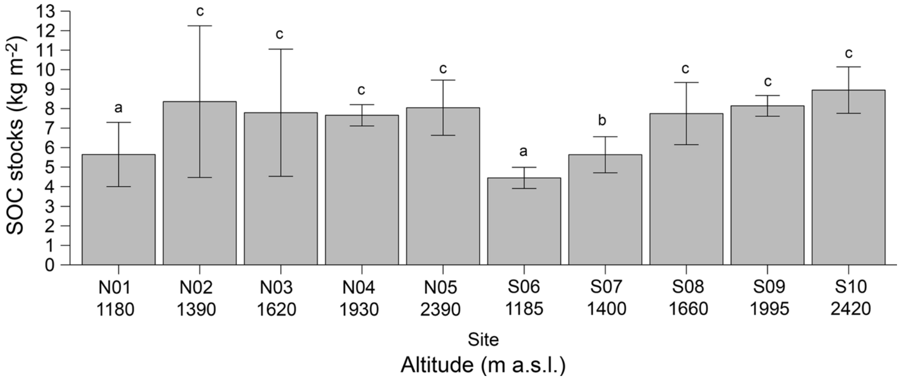

Fig. 2 Carbon stocks (0–15 cm) along the northern and southern altitudinal sequence. The *letters* indicate significant differences (p < 0.05)

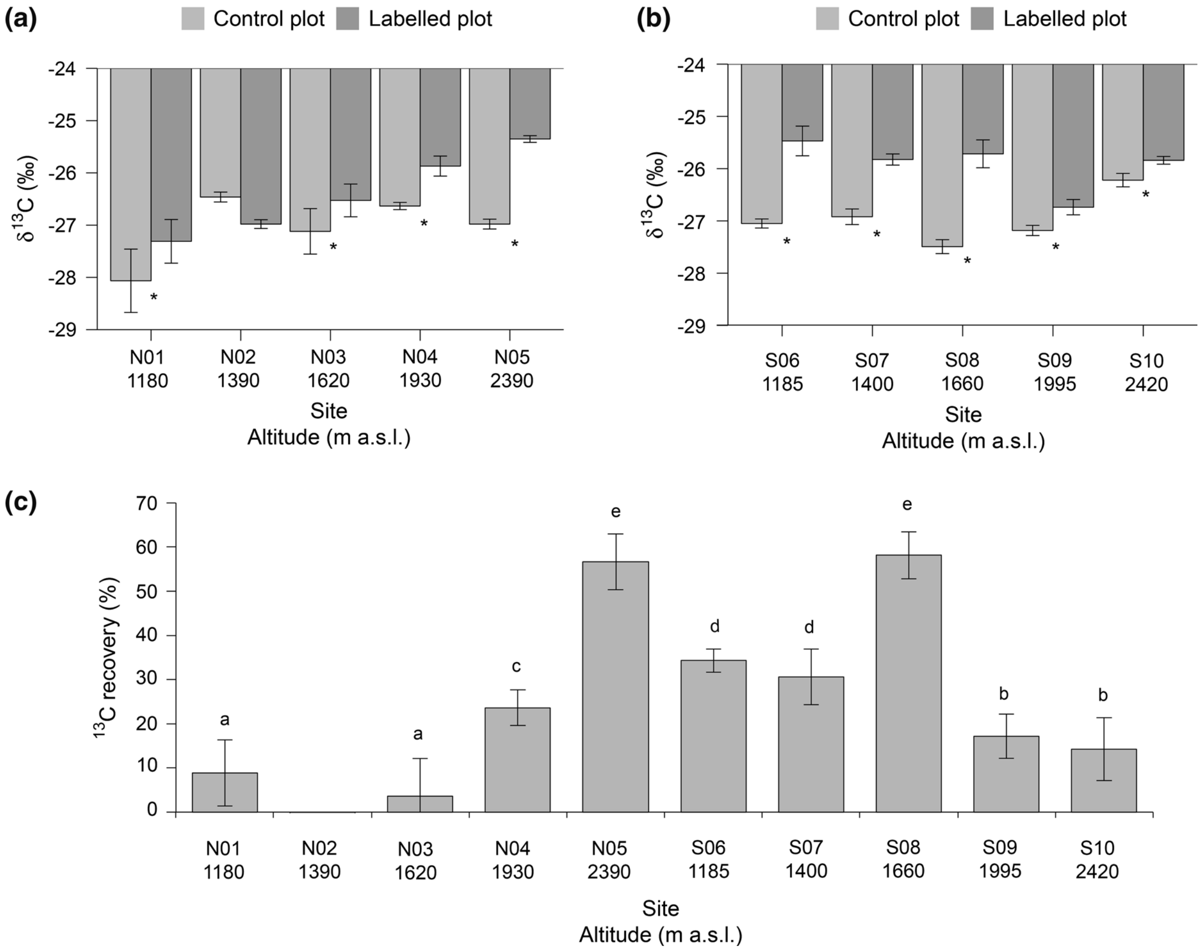

Fig. 3 δ^{13}C signal of the control and manipulated (addition of labelled Norway spruce needles) soil (0–5 cm) at the northern (**a**) and southern slope (**b**) and related site-specific ^{13}C recovery rates (**c**). *Asterisk* indicates significant differences (p < 0.05) between the light (LF) and heavy (HF) fraction, and letters differences along the altitudinal gradient and exposure

sequences were at a maximum of 1650 m a.s.l. (Fig 5b, c). C/N ratios were always lower in the heavy-density fraction ($p < 0.001$), especially in the north-facing sites.

In the 0–5 cm layer of control soils the δ^{13}C signal in the LF was distinctly more negative than the δ^{13}C signal in the HF ($p < 0.001$; Fig. 6a, b). Isotopic differences between LF and HF were significantly

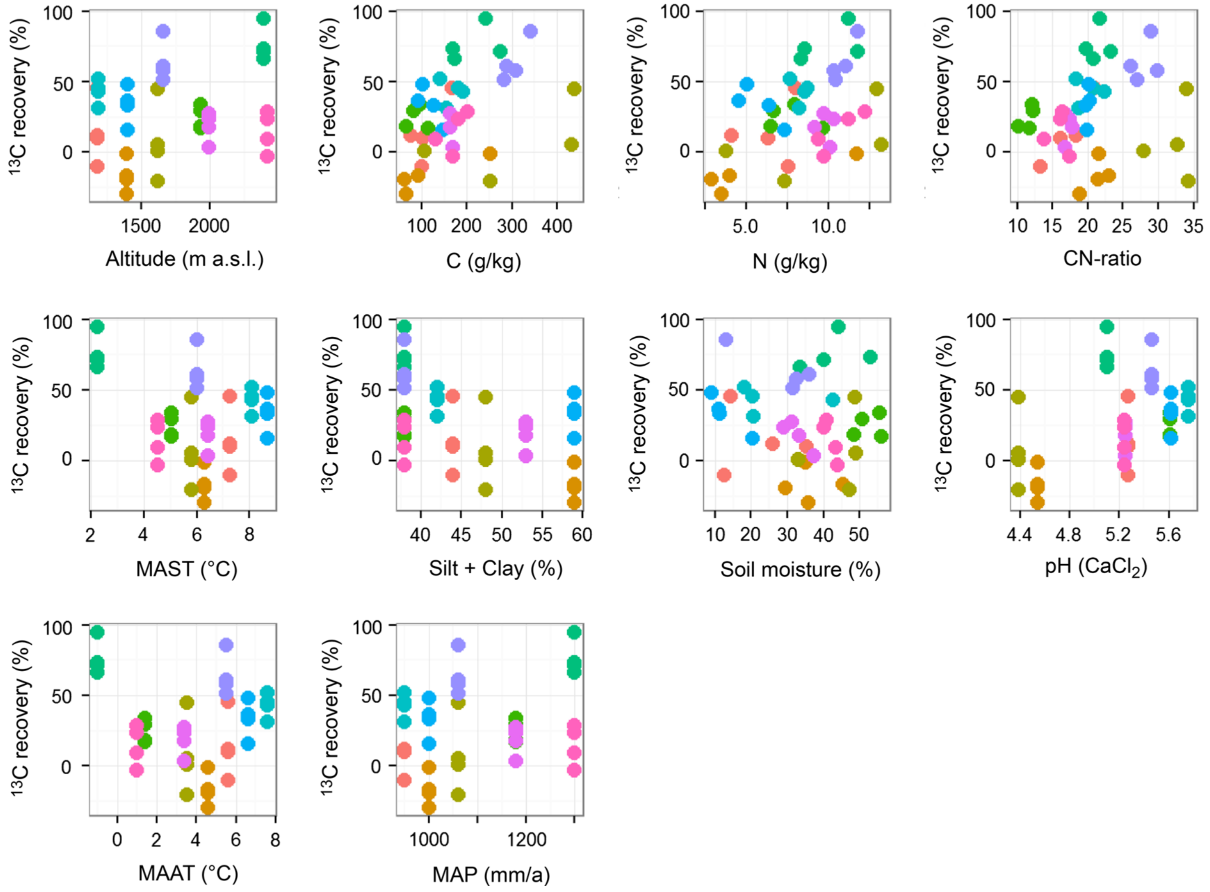

Fig. 4 Comparison between ^{13}C recovery and explanatory variables such as the altitude, org. C content, N-content, CN-ratio, mean annual soil temperature MAST, sum of silt and clay, soil moisture, pH, mean annual temperature MAAT and mean annual precipitation MAP. The *different colours* (points) refer to the individual sites

Table 3 Average correlation coefficients (±SD) obtained by data permutation (replicates) at each site. The ^{13}C recoveries (all sites, north-facing sites, south-facing sites) were related to several explanatory variables

	^{13}C recovery (all sites)		^{13}C recovery (north)		^{13}C recovery (south)	
	Cor	CorSD	Cor	CorSD	Cor	CorSD
Altitude	0.27	0.13	0.70*	0.18	−0.60*	0.20
Org. C	0.39	0.24	0.45	0.39	0.40	0.28
N	0.33	0.30	0.60	0.37	0.10	0.23
C/N-ratio	0.20	0.21	−0.20	0.40	0.85*	0.16
Soil temp.	−0.28	0.11	−0.70*	0.18	0.20	0.27
Silt and clay	−0.51*	0.10	−0.87*	0.14	−0.21	0.26
Soil moisture	−0.12	0.24	0.20	0.40	−0.50	0.34
pH	0.45	0.17	0.60	0.29	0.60*	0.19
MAAT	−0.14	0.12	−0.60*	0.20	0.60*	0.19
MAP	0.25	0.13	0.70*	0.20	−0.60*	0.17

*High (R ≥ 0.5) and stable (corSD ≤ 0.20) correlations

larger in soils of the southern than northern slope ($p = 0.018$; 1.27 ± 0.06‰ on southern vs 0.93 ± 0.11‰ on northern slopes). With labelling, significant differences to the control sites were detectable in the light fraction—especially at the sites N04, N05 and S06–S10 (Fig. 6a, b). These

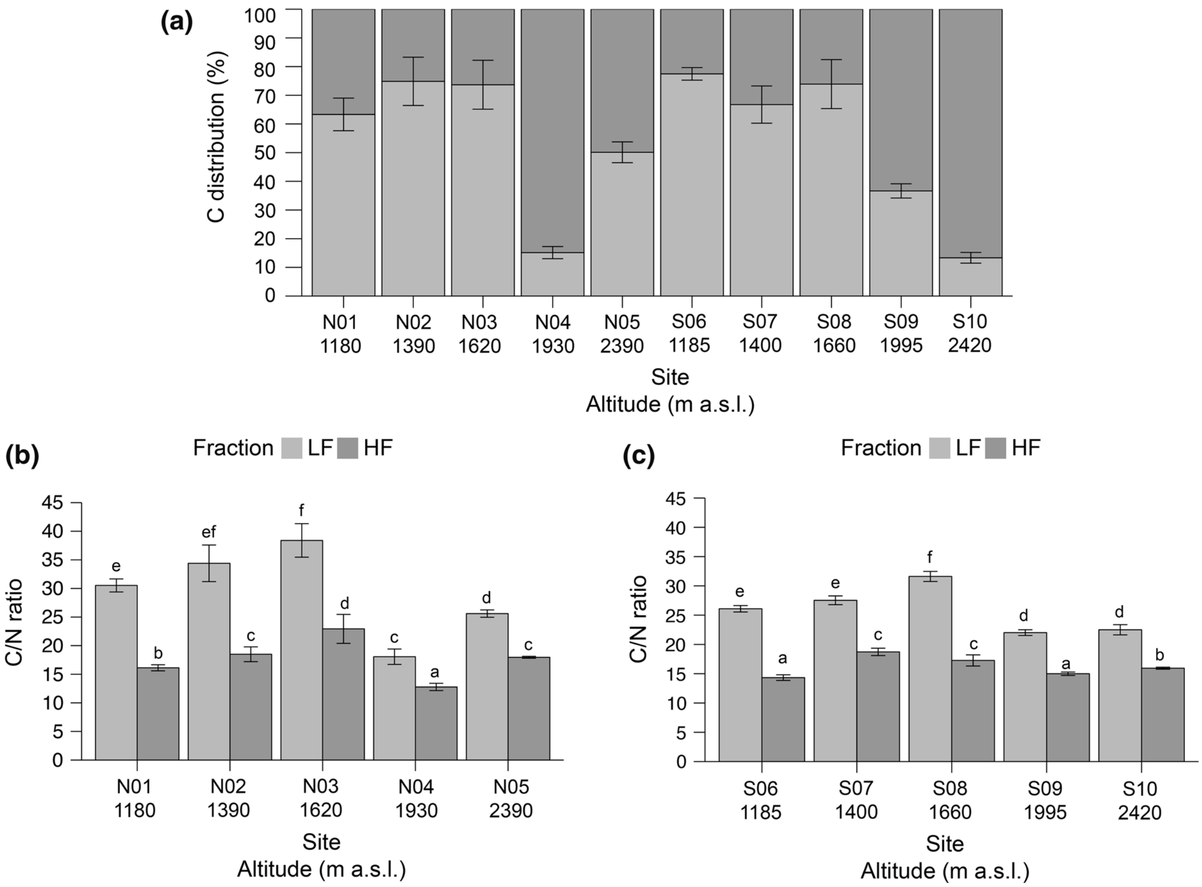

Fig. 5 Organic carbon distribution (0–5 cm depth) among the *light* and *heavy* fractions (**a**) and C/N ratios in the density fractions on the northern (**b**) and southern slope (**c**). *Asterisk* indicates significant differences ($p < 0.05$) between control and labelled plot and *letters* differences along the altitudinal gradient and exposure

differences were less pronounced in the heavy fraction (Fig. 6c, d).

Priming effect

A priming effect was not discernible or was very difficult to be detected. An average of 0.07 (± 0.23) kg C/m^2 on north-facing sites and 0.18 (± 38) kg C/m^2 on south-facing sites seemed to be lost due to a priming effect. These values, however, do not statistically differ from a zero-effect. The addition of 2 g of labelled OM to the mesocosms would have given rise to a maximal increase of +0.11 kg C/m^2 under the assumption that no C would have been mineralised.

Density fraction-specific ^{13}C recoveries

The fraction-specific recoveries of ^{13}C followed a similar trend as the ^{13}C recoveries of the bulk soil samples (Fig. 7a, b). Most of the sites had smaller ^{13}C recoveries in the HF than in the LF (sites: N03, N05, S06, S07, S08, S09 and S10; Fig. 7). ^{13}C recoveries increased with altitude on the north-facing sites but decreased with increasing altitude at the south-facing sites. The mean ^{13}C recovery at the north-facing sites was 13.2 ± 3.9% in the LF and 11.1 ± 2.5% in the HF. At the south-facing sites the average recovery was higher in the LF (25.2 ± 4.0%) and slightly lower % in the HF (9.3 ± 1.8%). With respect to the recovered ^{13}C, the

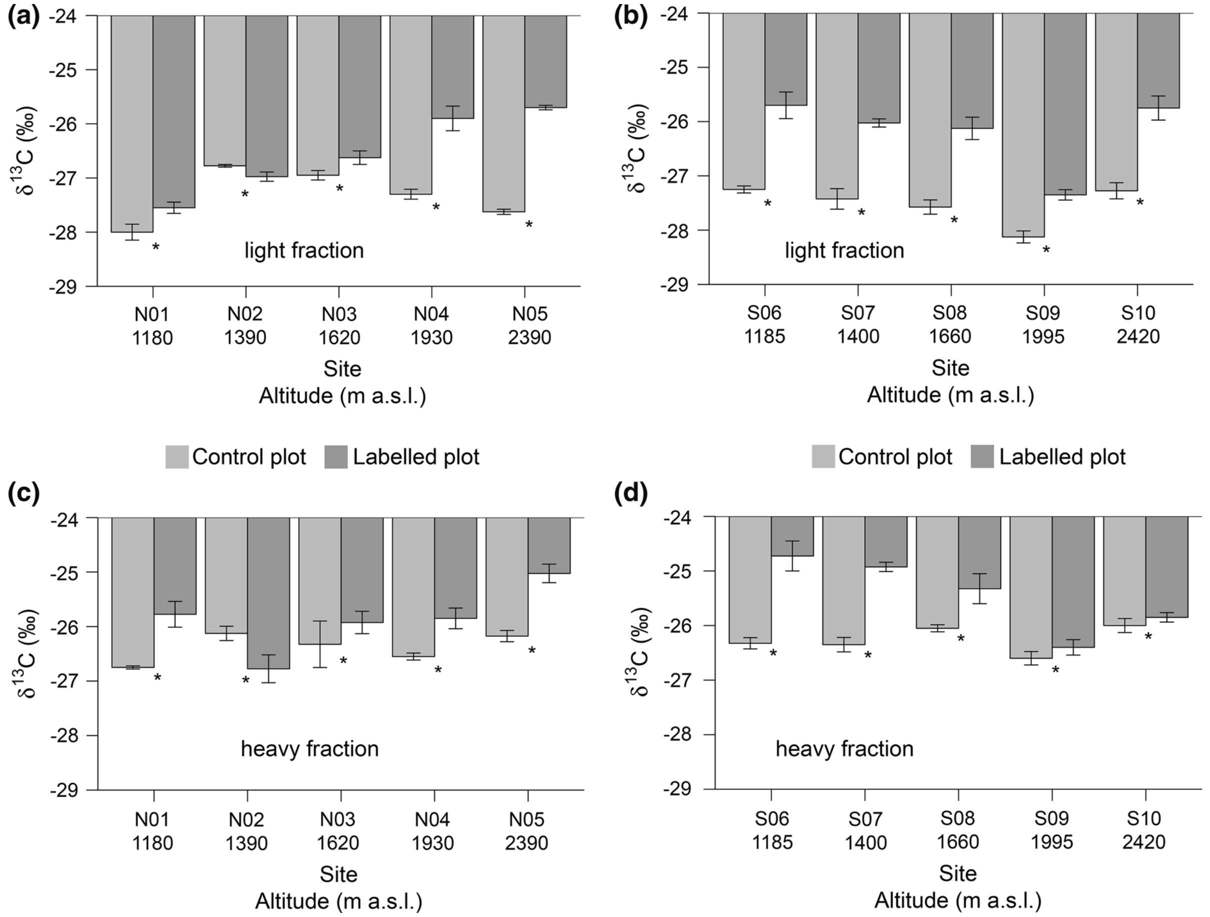

Fig. 6 Comparison of the $\delta^{13}C$ signature in the soil (0–5 cm) of the control and *labelled plots* with respect to the light fraction at the north-facing (**a**) and south-facing slope (**b**) and with respect to the heavy fraction at the north-facing (**c**) and south-facing slope (**d**). *Asterisk* indicates significant differences ($p < 0.05$) between control and labelled plot

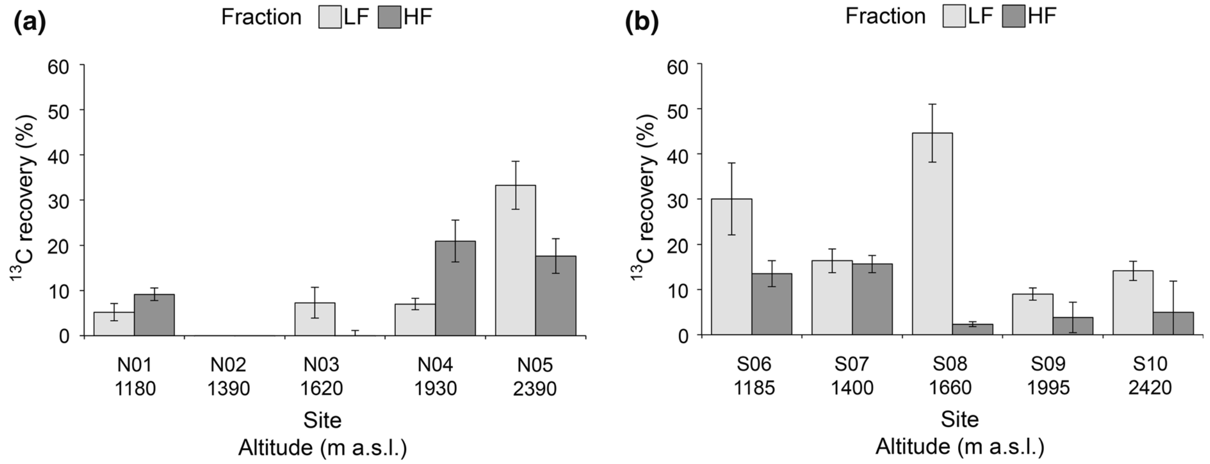

Fig. 7 ^{13}C recoveries (of Norway spruce needles after one year) in 0–5 cm soil depth in the low (LF) and high density (HF) fraction of the north-facing (**a**) and south-facing sites (**b**)

average found at the north-facing sites was 54% in the LF and 46% in the HF and at the south-facing sites was 73% in the LF and 27% in the HF. The ^{13}C recoveries in the light fraction at the northern slope were significantly ($p = 0.005$) lower than at the south-facing sites. The ^{13}C recoveries in the heavy fraction did not seem to be affected by exposure.

Discussion

SOC concentrations and stocks

Both altitudinal sequences exhibited high but also strongly varying SOC concentrations, which is characteristic of soils in such environments (Table 1; Egli et al. 2006, 2009; Garcia-Pausas et al. 2007; Djukic et al. 2010). Interestingly, the SOC concentrations were highest at the north-facing site close to the timberline, which may be explained by a similarly high C input but reduced microbial activity compared to the rest of the forest (due to climatic restrictions and the low pH; Davidson and Janssens 2006). This regime of greatest SOC concentrations close to the timberline is typical for Alpine regions (Egli et al. 2009). A comparable trend can also be detected for the C/N ratio, which reached a maximum at this altitude (1650 m a.s.l.). Furthermore, the C/N ratios of the south-facing sites were significantly lower at the soil depths 5–10 and 10–15 cm compared to the north-facing sites indicating either a better association of SOC to minerals or a more favourable substrate for decomposition (Kleber et al. 2007). The measured SOC stocks along the altitudinal sequence were similar to that which has been reported by Rodeghiero and Cescatti (2005) in the Italian Alps, Garcia-Pausas et al. (2007) in the Pyrenees, Dahlgren et al. (1997) in the western Sierra Nevada and Garten and Hanson (2006) in the Appalachian Mountains. A number of studies indicate increasing SOC stocks with increasing altitudes (Garcia-Pausas et al. 2007; Garten and Hanson 2006). Others found a U-shaped trend having a maximum SOC stock close to the treeline (Dahlgren et al. 1997; Djukic et al. 2010; Rodeghiero and Cescatti 2005). We, however, have to take into account that the presented stocks here only referred to a soil depth of 0–15 cm and are therefore not complete.

Overall ^{13}C recovery

The patterns of ^{13}C recovery with respect to environmental factors show the importance of temperature and moisture as drivers. Similar to Murphy et al. (1998), a decreasing litter mass recovery with increasing altitude was found for the south-facing slopes (Table 3). However, rather the opposite would have been expected: with decreasing temperature the decomposition rate of OM would usually be expected to be lower. Another surprising observation is that ^{13}C recovery at the north-facing sites was lower than at the southern gradient—but only at altitudes up to about 1700 m a.s.l. (Fig 3c). At higher altitudes, the opposite was measured. These trends are most likely governed by two factors: temperature and moisture availability. Soil moisture (Table 2) was indeed lower at south-facing sites at altitudes $<$1700 m a.s.l. ($p < 0.01$). Water availability in soils is a driving factor of decomposition (Davidson and Janssens 2006). The presence of the humus form Amphi (Table 1) on south-facing sites is a morphological expression of the drier conditions. At the high-alpine sites, however, temperature becomes more and more the dominant factor and differences in soil moisture between the north- and south-facing sites were negligible. As a consequence, the highest and coldest north-facing sites had a higher C recovery. We therefore propose that OM decomposition at the north-facing sites strongly depends on temperature while at the south-facing sites, moisture availability is a more prominent factor. Soil acidity is a key driver for the turnover of organic matter in cold areas (Leifeld et al. 2013). It exerts a strong control on residue decomposition and transport of OC within the soil profile. Such a relationship is indicated by the relatively high correlation coefficient between ^{13}C recovery and pH (Table 3). These results are in agreement with Fravolini et al. (2016) who found that a higher (soil) moisture and clay content along with a lower pH seemed to accelerate wood decay in these environments.

Methodological difficulties with ^{13}C recoveries

Diverse approaches to measure ^{13}C recoveries have been used in literature. Among these approaches are isotope-labelling techniques, litterbag experiments, different applied substrates, incomparable climatic

Table 4 Overview of different litter decomposition studies

Source	Location	Method	Substrate	Time span	Results (C or mass recovery)
Present Study	Trentino, Italy	Stable isotopes	Norway spruce needles	12 month	18.5 ± 5.3% (N-slopes; C) 31.5 ± 5.3% (S-slopes; C)
Bird et al. (2008)	Sierra Nevada, USA	Stable isotopes	Pine needles	24 month	18.1 ± 2.7% (C)
Bottner et al. (2000)	France	Stable isotopes	Wheat residues	12 month	35% (C)
Rubino et al. (2010)	Tuscany, Italy	Stable isotopes	Black poplar foliage	11 month	20.0 ± 3.0% (C)
Kammer and Hagedorn (2011)	Lägern, Switzerland	Stable isotopes	Beech foliage	12 month	23–31% (C)
Hatton et al. (2015)	Georgetown CA, USA	Stable isotopes	Ponderosa pine	57.5 month	37–39% (C); after 1 year: 49% (C)
Kammer and Hagedorn (2011)	Lägern, Switzerland	Litter bag (mass loss)	Beech foliage	12 month	67.5% (mass)
Murphy et al. (1998)	Arizona, USA	Litter bag (mass loss)	Different Pine needles	12 month	75–85% (mass)
Lorenz et al. (2000)	Black Forest, Germany	Litter bag (mass loss)	Norway spruce needles	12 month	77.5 ± 2.4% (mass)
Lorenz et al. (2000)	Ontario, Canada	Litter bag (mass loss)	Norway spruce needles	12 month	78.6 ± 4.4% (mass)

conditions and rarely altitudinal sequences. Sometimes the necessary details are lacking to trace back how the calculation of carbon recovery was performed. In addition, it seems that the dilution effect of the substrate added to a soil was not always taken into account. Some litterbag and stable-isotope investigations are compiled in Table 4. Interestingly, all the listed isotopic experiments showed results that are similar to our study, although there were climatic differences and different litter substrates applied (Table 4). Kammer and Hagedorn (2011) found that litterbags gave two to three times higher substrate recoveries compared to the isotope-labelling approach. According to Kammer and Hagedorn (2011), litter bags may lose material and preferentially select the meso-fauna (owing to the size of the mesh). As a consequence, the litter decomposition is affected. The contribution of labelled litter to carbon fluxes can be obtained by measuring the CO_2 efflux and its $\delta^{13}C$ signature, soil water and/or by comparing the $\delta^{13}C$ of soil and added litter (Kammer and Hagedorn 2011; Hatton et al. 2015). The type of decomposition processes and involved (macro- and micro) organisms may vary between soil horizons (or soil depth) and even shift during decomposition (Ascher et al. 2012; van der Wal et al. 2016). This variability cannot be taken into account when measuring an overall CO_2 efflux or when only considering one soil depth interval that may overlap with two or more soil horizons.

Priming effect

A negative priming effect (PE_{stock}; Eq. 5) characterises an extra decomposition of SOC after addition of an easily-decomposable substrate to the soil due to a stimulated mineralisation rate of soil microorganisms (Kuzyakov et al. 2000). Depending on the substrate added it is possible that the supply of degradable SOM increases the population of the SOM-feeding microbes, which can survive even after the substrate was exhausted (Fontaine et al. 2004). In contrast, it is also possible that the added substrate may inhibit SOM decomposition (Fontaine et al. 2004). The priming effect measured in this study did not significantly differ from a zero-effect. Consequently, a major priming effect can be excluded.

Tracking the traces of carbon during decay

Equations 3 and 4 enabled the calculation of how much of the initial litter substrate is recovered in each soil compartment (Fig. 7a, b). The ^{13}C recoveries of

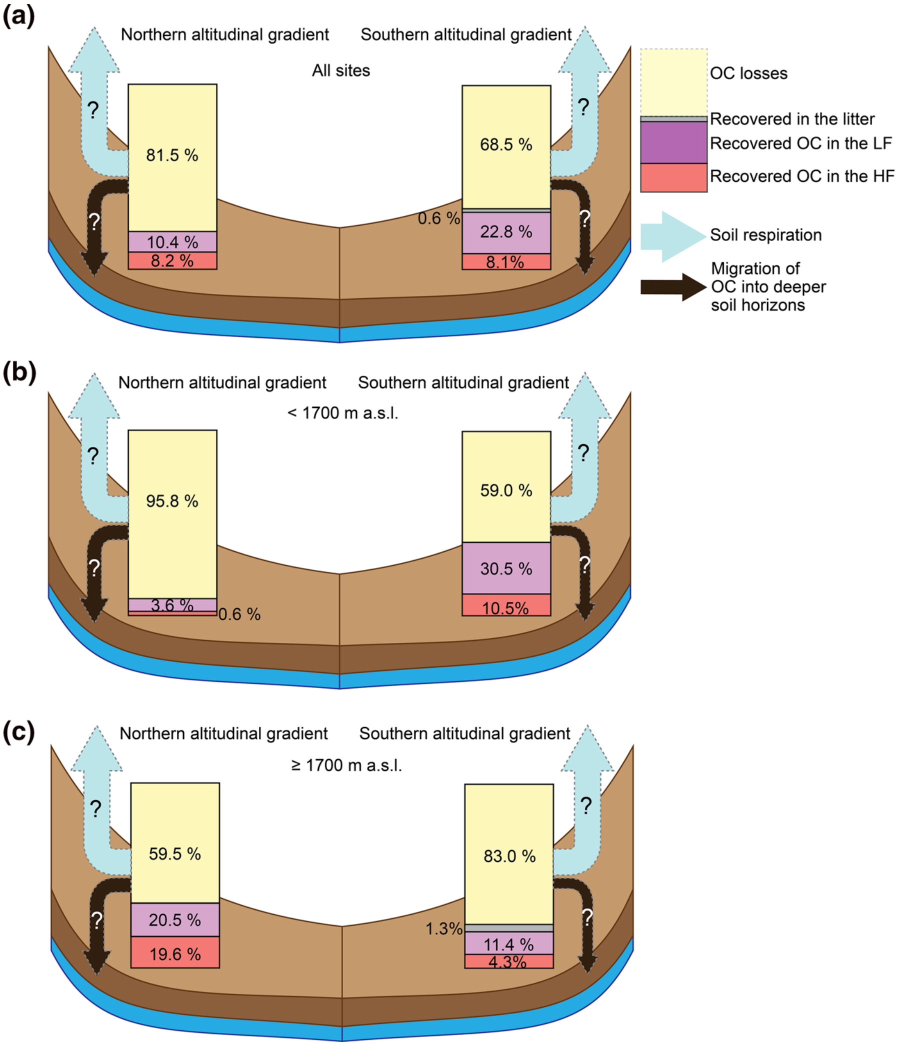

Fig. 8 Average carbon mass balance (after 1 year) of the added Norway spruce needle substrate of the northern and southern altitudinal sequence (0–5 cm). Organic carbon losses are due to soil respiration, migration to deeper soil horizons and the leaching of dissolved organic carbon (DOC). The carbon recovery is given for the light (LF), heavy fraction (HF) and litter

both fractions (LF and HF) in general showed increasing values with increasing altitude at the northern slope, whereas the southern slope was characterised by a rather decreasing trend. At the south-facing sites, higher recoveries for the LF were measured compared to the HF. HF is most commonly characterised by having reactive minerals such as clay minerals and oxyhydroxides that have the potential to chemically interact with organic compounds and stabilise them (Sollins et al. 2006; Hatton et al. 2012).

Hatton et al. (2015) detected that needle-derived C placed in the A horizon was redistributed toward slow-cycling SOM fractions (which corresponds to HF)—unlike the needle-derived C placed in the O horizon, which lacks significant mineral stabilisation mechanisms. Although some of our sites (those at the highest elevation) had a major proportion of a mineral A-horizon, it seems rather unlikely that a large proportion of the added OM had distinct chemical interactions with minerals, since a major part was lost and the recovered part was predominantly found in the light fraction (Fig. 8a–c). Such an observation is in agreement with Bird et al. (2008) and Singh et al. (2014) who reported distinctly larger ^{13}C recoveries in the LF compared to the HF. On average, 8.2 ± 2.4% of the applied ^{13}C (i.e., 43% of the recovered C) seemed to be stabilised in the HF at the north-facing sites and the same amount 8.1 ± 1.8% (i.e., 26% of the recovered C) at the south-facing sites (Fig. 8a). Since the southern slope showed higher soil temperatures, we expected a faster OM decomposition and smaller ^{13}C recoveries due to a higher microbial activity at higher soil temperatures (Davidson et al. 2006). Although the climate in the investigated valley can be considered as humid, water scarcity due to evapotranspiration, particularly in summer and early autumn, seems to inhibit OM decay at the south-facing sites (Fig. 8b). An alternative explanation is given by Frey et al. (2013) who found that the efficiency with which soil microorganisms use organic matter is dependent on both temperature and substrate quality, with efficiency declining with increasing temperatures for more recalcitrant substrates. At sites $\geq$1700 m a.s.l., however, this situation changes and the ^{13}C-recoveries were higher at the north-facing sites (Fig. 8b, c). As a consequence, soil temperature correlated negatively ($p < 0.05$) with the ^{13}C recovery (particularly in the LF) at the northern slopes, while a contrary effect was detected at the southern slopes.

Carbon losses can occur over soil respiration, leaching of OC into deeper horizons (in a dissolved or particulate form) or via transfer into the litter layer. This last process is nonexistent to marginal (Fig. 8a–c). During the experiment, the discrimination of ^{13}C against ^{12}C seems to have been more pronounced at the southern slope. Consequently, soil respiration of OM might have been higher at the south-facing sites compared to the north-facing sites (Powers and Schlesinger 2002). If this is the case, then the higher overall C losses on the northern slope can only be explained by leaching export of dissolved OM: a hypothesis that cannot be further checked, because the corresponding data is missing. Furthermore, the lower pH values at the north-facing sites restrict respiration to a certain extent (Leifeld et al. 2013) and promote leaching. Egli et al. (2006, 2009) showed that north-facing sites in these Alpine environments have more intense leaching conditions (podzolisation). Typical podzolisation processes are detectable along the whole sequence of northern sites but only above 2000 m a.s.l. on south-facing sites. The development of smectites in the clay fraction reflects this weathering behaviour; this mineral was discernible in the surface horizon particularly on the north-facing slopes (Egli et al. 2006) in the sub-alpine climate zone. On the south-facing sites, smectitic components were only detected in the high-alpine climate zone (Egli et al. 2006). We therefore speculate that the more acidic, moister and cooler conditions on the north-facing sites have increased the removal of decay products of spruce needle OM via soil water (leaching).

Conclusions

Slope exposure (microclimate) is often a neglected factor when studying the decay of OM. In the investigated Alpine area, microclimatic effects distinctly determined the decay processes of OM. At altitudes below 1700 m a.s.l., water scarcity diminished the decay rate of OM at south-facing sites—this although the climate is humid. At altitudes >1700 m a.s.l., however, the situation changed and soil moisture was no longer a limiting factor and the influence of temperature became a more dominant factor. Although moisture availability and temperature are crucial, additional factors such as the grain size, pH and podzolisation (which contributes to an increased leaching of OM) interfered with OM decay and stabilisation.

Labelling experiments in the field using mesocosms enabled the fate of carbon derived from Norway spruce needles to be traced back. Although this approach has its limitations (costly, fixed soil depth, etc.), labelling experiments have advantages over litter bag approaches where material may be lost or the meso-fauna (as part of the decomposer community) preferentially selected.

Acknowledgements This study is part of the DecAlp DACH project no. 205321L_141186 and the snf project 200021_162338. J. Ascher-Jenull has been funded by the Fonds zur Förderung der wissenschaftlichen Forschung (FWF) Austria (Project I989-B16). We are indebted to Fabio Angeli of the 'Ufficio distrettuale forestale di Malé' and his team of foresters for their support in the field.

References

Ascher J, Sartori G, Graefe U, Thornton B, Ceccherini MT, Pietramellara G, Egli M (2012) Are humus forms, mesofauna and microflora in subalpine forest soils sensitive to thermal conditions? Biol Fertil Soils 48:709–725

Bernoux M, Cerri CC, Neill C, de Moraes JF (1998) The use of stable carbon isotopes for estimating soil organic matter turnover rates. Geoderma 82:43–58

Bird JA, Kleber M, Torn MS (2008) ^{13}C and ^{15}N stabilization dynamics in soil organic matter fractions during needle and fine root decomposition. Org Geochem 39:465–477

Bottner P, Coûteaux MM, Anderson JM, Berg B, Billès G, Bolger T, Casabianca H, Romanyá J, Rovira P (2000) Decomposition of ^{13}C-labelled plant material in a European 65°–40° latitudinal transect of coniferous forest soils: simulation of climate change by translocation of soils. Soil Biol Biochem 32:527–543

Cerli C, Celi L, Kalbitz K, Guggenberger G, Kaiser K (2012) Separation of light and heavy organic matter fractions in soil—testing for proper density cut-off and dispersion level. Geoderma 170:403–416

Dahlgren RA, Rasmussen C, Southard RJ (1997) Soil development along elevational transects on granite, andesitic lahar and basalt in the western Sierra Nevada, California. Geoderma 78:207–236

Davidson EA, Janssens IA (2006) Temperature sensitivity of soil carbon decomposition and feedbacks to climate change. Nature 440:165–173

Davidson EA, Janssens IA, Lou Y (2006) On the variability of respiration in terrestrial ecosystems: moving beyond Q10. Glob Change Biol 12:154–164

Djukic I, Zehetner F, Tatzber M, Gerzabek MH (2010) Soil organic-matter stocks and characteristics along an Alpine elevation gradient. J Plant Nutr Soil Sci 173:30–38

Egli M, Mirabella A, Sartori G, Zanelli R, Bischof S (2006) Effect of north and south exposure on weathering rates and clay mineral formation in Alpine soils. Catena 67:155–174

Egli M, Sartori G, Mirabella A, Favilli F, Giaccai D, Delbos E (2009) Effect of north and south exposure on organic matter in high Alpine soils. Geoderma 149:124–136

Fontaine S, Bardoux G, Benest D, Verdier B, Mariotti A, Abbadie L (2004) Mechanisms of the priming effect in a Savannah soil amended with cellulose. Soil Sci Soc Am J 68:125–131

Frey SD, Lee J, Melillo JM, Six J (2013) The temperature response of soil microbial efficiency and its feedback to climate. Nat Clim Change 3:395–398

Garcia-Pausas J, Casals P, Camarero L, Huguet C, Sebastià MT, Thompson R, Romanyà J (2007) Soil organic carbon storage in mountain grasslands of the Pyrenees: effects of climate and topography. Biogeochemistry 82:279–289

Garten CTJ, Hanson PJ (2006) Measured forest soil C stocks and estimated turnover times along an elevation gradient. Geoderma 136:342–352

Hatton PJ, Kleber M, Zeller B, Moni C, Plante AF, Townsend K, Gelhaye L, Lajtha K, Derrien D (2012) Transfer of litter-derived N to soil mineral-organic associations: evidence from decadal ^{15}N tracer experiments. Org Geochem 42:1489–1501

Hatton PJ, Castanha C, Torn MS, Bird JA (2015) Litter type control on soil C and N stabilization dynamics in a temperate forest. Glob Change Biol 21:1358–1367

Jabiol B, Zanella A, Ponge JF, Sartori G, Englisch M, van Delft D, de Waal R, Le Bayon RC (2013) A proposal for including humus forms in the World Reference Base for Soil Resources (WRB-FAO). Geoderma 192:286–294

Kammer A, Hagedorn F (2011) Mineralisation, leaching and stabilisation of ^{13}C-labelled leaf and twig litter in a beech forest soil. Biogeosciences 8:2195–2208

Kleber M, Sollins P, Sutton R (2007) A conceptual model of organo-mineral interactions in soils: self-assembly of organic molecular fragments into zonal structures on mineral surfaces. Biogeochemistry 85:9–24

Kuzyakov Y, Friedel JK, Stahr K (2000) Review of mechanisms and quantification of priming effects. Soil Biol Biochem 32:1485–1498

Leifeld J, Bassin S, Conen F, Hajdas I, Egli M, Fuhrer J (2013) Control of soil pH on turnover of belowground organic matter in subalpine grassland. Biogeochemistry 112:59–69

Liski J, Nissinen A, Erhard M, Taskinen O (2003) Climatic effects on litter decomposition from arctic tundra to tropical rainforest. Glob Change Biol 9:575–584

Lorenz K, Preston CM, Raspe S, Morrison IK, Feger KH (2000) Litter decomposition and humus characteristics in Canadian and German spruce ecosystems: information from tannin analysis and ^{13}C CPMAS NMR. Soil Biol Biochem 32:779–792

Maestrini B, Abiven S, Singh N, Bird JA, Torn MS, Schmidt MWI (2014) Carbon losses from pyrolysed and original wood in a forest soil under natural and increased N deposition. Biogeosciences 11:5199–5213

Murphy KL, Klopatek JM, Klopatek CC (1998) The effects of litter quality and climate on decomposition along an elevational gradient. Ecol Appl 8:1061–1071

Patruno A, Cavazza L, Castriganò A (1997) Metodi di analisi fisica del suolo, Parte III, 1. Ministero per le Politiche Agricole Osservatorio Nazionale Pedologico e per la Qualità del suolo, in collaborazione con International Society of Soil Science, ISO/DIS 11277

Petrillo M, Cherubini P, Sartori G, Abiven S, Ascher J, Bertoldi D, Barbero A, Larcher R, Egli M (2015) Biochemical characteristics of decomposing deadwood in an Alpine forest and their relation to climate. iForest 9:154–164

Powers JS, Schlesinger WH (2002) Geographic and vertical patterns of stable carbon isotopes in tropical rain forest soils of Costa Rica. Geoderma 109:141–160

Rodeghiero M, Cescatti A (2005) Main determinants of forest soil respiration along an elevation/temperature gradient in the Italian Alps. Glob Change Biol 11:1024–1041

Rubino M, Dungait JAJ, Evershed RP, Bertolini T, De Angelis P, D'Onofrio A, Lagomarsino A, Lubritto C, Merola A, Terrasi F, Cotrufo MF (2010) Carbon input belowground is the major C flux contributing to leaf litter mass loss: evidences from a ^{13}C labelled-leaf litter experiment. Soil Biol Biochem 42:1009–1016

Sboarina C, Cescatti A (2004) Il clima del Trentino—Distribuzione spaziale delle principali variabili climatiche. Report 33, Centro di Ecologia Alpina Monte Bondone, Trento, Italy

Schmid MO, Gubler S, Fiddes J, Gruber S (2012) Inferring snowpack ripening and melt-out from distributed measurements of near-surface ground temperatures. Cryosphere 6:1127–1139

Schmidt MWI, Torn MS, Abiven S, Dittmar T, Guggenberger G, Janssens IA, Kleber M, Kögel-Knabner I, Lehmann J, Manning DAC, Nannipieri P, Rasse DP, Weiner S, Trumbore SE (2011) Persistence of soil organic matter as an ecosystem property. Nature 478:49–56

Schulze ED, Wirth C, Heimann M (2000) Managing forests after Kyoto. Science 289:2058–2059

Singh N, Abiven S, Maestrini B, Bird JA, Torn MS, Schmidt MWI (2014) Transformation and stabilization of pyrogenic organic matter in a temperate forest field experiment. Glob Change Biol 20:1629–1642

Sollins P, Swanston C, Kleber M, Filley T, Kramer M, Crow S, Caldwell BA, Lajtha K, Bowden R (2006) Organic C and N stabilization in a forest soil: evidence from sequential density fractionation. Soil Biol Biochem 38:3313–3324

Studer MS, Siegwolf RTW, Abiven S (2014) Carbon transfer, partitioning and residence time in the plant-soil system: a comparison of two $^{13}CO_2$ labelling techniques. Biogeosciences 11:1637–1648

van der Wal A, Klein Gunnewiek PJA, Cornelissen JHC, Crowther TW, de Boer W (2016) Patterns of natural fungal community assembly during initial decay of coniferous and broadleaf tree logs. Ecosphere 7:1–17

Zanella A, Jabiol B, Ponge JF, Sartori G, De Waal R, Van Delft B, Graefe U, Cools N, Katzensteiner K, Hager H, Englisch M (2011) A European morpho-functional classification of humus forms. Geoderma 164:138–145